11-15-2000

Infrared switching electrochromic devices based on tungsten oxide

E. B. Franke
University of Nebraska-Lincoln, efranke3@unl.edu

C. L. Trimble
University of Nebraska-Lincoln

J. S. Hale
J. A. Woollam Co.

Mathias Schubert
University of Nebraska-Lincoln, mschubert4@unl.edu

John A. Woollam
University of Nebraska-Lincoln, jwoollam1@unl.edu

Infrared switching electrochromic devices based on tungsten oxide

E. B. Franke[a)]

*Center for Microelectronic and Optical Materials Research, and Department of Electrical Engineering,
University of Nebraska, Lincoln, Nebraska 68588-0511 and Institut für Oberflächenmodifizierung Leipzig
e.V., Permoserstrasse 15, 04318 Leipzig, Germany*

C. L. Trimble

*Center for Microelectronic and Optical Materials Research and Department of Electrical Engineering,
University of Nebraska, Lincoln, Nebraska 68588-0511*

J. S. Hale

J. A. Woollam Co., Inc., Suite 102, 645 M Street, Lincoln, Nebraska 68588

M. Schubert and J. A. Woollam

*Center for Microelectronic and Optical Materials Research, and Department of Electrical Engineering,
University of Nebraska, Lincoln, Nebraska 68588-0511*

Different types of electrochromic devices for thermal emittance modulation were developed in the
spectral region from mid- to far-infrared (2–40 μm). In all devices polycrystalline and amorphous
tungsten oxide have been used as electrochromic and ion storage layer, respectively. Two types of
all-solid-state devices were designed, one with a metal grid for the top and bottom electrode
deposited on a highly emissive glass substrate, and another with a top metal grid electrode and a
highly reflecting bottom metal electrode layer. Tantalum oxide is used as an ion conductor in both
device types. The third device type consists of a polymeric ion conductor. All solid-state constituent
layers were grown by either reactive or nonreactive dc or rf magnetron sputtering in a high vacuum
environment. Modulation of the emittance is accomplished by reversible insertion of Li ions into
polycrystalline WO_3 by applying and switching a small voltage across the structure. Spectrally
dependent measured reflectance modulation of the device has been used to determine the device
emissivity modulation with respect to the blackbody emissivity spectra at 300 K. Best device
performance was found in both solid-state devices showing an emissivity modulation of about 20%.
© *2000 American Institute of Physics.* [S0021-8979(00)01623-6]

I. INTRODUCTION

Electrochrochromic materials have the peculiarity to
change reversibly the optical properties (refractive index n,
extinction coefficient k) upon insertion and extraction of
small ions after application of small voltages. Many materials
are known to show electrochromic behavior, and tungsten
trioxide is the most extensively studied electrochromic material.
This electrochromic behavior can be used for many
applications. In recent years electrochromic devices (ECD)
have been primarily investigated for use in the visible spectral
region. Applications include transmittance modulation of
sunlight control window glazings for buildings (smart windows),
optical displays, and reflectance modulating automobile
rear-view mirrors.[1]

Electrochromic devices can also be used for surface
emissivity control [emissivity modulation devices (EMD)].
Surface emissivity characteristics are represented by the
blackbody spectra at a defined temperature. EMDs are especially
of interest for thermal control in satellites.[2–4] Thermal
control of satellites is accomplished by balancing the energy
dissipated by satellite electrical components against the energy
emitted as IR radiation.[5] Satellite emittance is charac-
terized by a blackbody spectrum at $T = 300$ K which has its
intensity maximum near 10 μm, if the satellite temperature is
aimed at room temperature. The EMD should have the highest
dynamic modulation in this spectral region.

Polycrystalline tungsten oxide can be used as an electrochromic
layer for infrared EMDs. According to Goldner
et al., and Cogan *et al.*[6–8] the emittance modulation occurs
by varying the concentration of free electrons during element
oxidation and reduction upon ion insertion and extraction,
respectively. Therefore the change in the emittance is controlled
by reflectance modulation. Amorphous tungsten oxide
can be used as an ion storage layer in EMDs. The amorphous
electrochromic material is usually transparent in a wide IR
spectral region, regardless of the inserted ion concentration.[9]

EMDs are multilayered, and structured as follows:
substrate/transparent electrode/ion storage layer/ion
conductor/electrochromic layer/transparent electrode. In our
devices small ions (typically H^+ or alkali ions) are introduced
into the device structure via an electrochemical process.
The ions are able to move from the electrochromic into
the ion storage layer and back again, driven by a voltage
applied between the electrodes. Electrochromic and ion storage
layers can be of complementary electrochromic behavior,
but the ion storage layer should be at least optically
stable upon ion insertion/extraction. Electrochromism is

[a)]Electronic mail: franke@engrs.unl.edu

complementary: The electrochromic layer is in its colored (bleached) state, and the ion storage layer is in its bleached (colored) state after ion insertion (extraction). Here, bleached and colored refer to the high and low optical transmission state of the material, respectively. The material quality of the ion conductor plays an important role for device performance. This layer should be a good conductor for small ions and a barrier for electrons. Electrochromic devices which operate in the visible to near-infrared spectral region (0.4–2.4 μm) are already commercially available.

So far electrochromic devices for the infrared (IR) especially for spectral regions at higher wavelength than the sun thermal emittance spectra have been much less investigated than electrochromics for the visible spectral region applications.[10,11] This may be due to special requirements needed for devices operating in the IR. For instance electrode materials transparent to visible light [indium tin oxide (ITO)] are highly reflective in the IR spectral region. This is directly related to the free carrier concentration of the material. Typically electrodes for the IR consist of highly conducting metal grids having at least 90% transmittance. Two different types of emittance modulation devices have been suggested. One type proposed by Baucke *et al.*[12] uses a highly reflecting bottom electrode and a highly transmitting top metal grid electrode. Here the emittance modulation is related to the reflectance modulation of the device. Topart *et al.*[13] and Trimble *et al.*[14] reported on modified devices of this general type, using polymers as ion conducting materials.

Cogan *et al.*[15] designed an emittance modulation device using two IR transparent electrode grids as bottom and top electrodes. The bottom electrode was deposited on a highly emissive substrate and a polymer was used as an ion conductor.

In this article we report on the structural design of three different EMD types, two all-solid state devices, and one polymer based device, as follows:

(1) An all-solid-state device with metal grids as bottom and top electrode materials on a highly emissive glass substrate.

(2) An all-solid-state device with a highly reflecting bottom metal electrode and a transparent top metal grid electrode.

(3) A polymer ion conductor based device using a AMPS/DMA copolymer saturated with $LiClO_4$. The polymer devices also contained diamondlike carbon (DLC) as antireflecting coatings on top of the slightly doped silicon electrode.

For all devices, polycrystalline (c) $Li_xW_{1-x}O_3$ and amorphous (a) $Li_xW_{1-x}O_3$ (or NiO) were used as the electrochromic and an ion storage layer, respectively. Tantalum oxide is used as an ion conductor in all-solid state devices. All constituent layers were deposited as single films on silicon or glass substrates and characterized by x-ray diffraction and variable angle spectroscopic ellipsometry to obtain crystal structure and optical properties. The operational properties were investigated for emittance modulation in the spectral region from 2 to 40 μm. The devices were based on reflectivity/emissivity modulation. We show results of simulated optical modulation for specific device structures. Cal-

TABLE I. Growth parameters used for electrochromic device constituents deposition.

Thin film	Deposition	p (mTorr)	t (°C)	f_{Ar} (sccm)	f_{O_2} (sccm)	d (nm)
ITO	45 W (dc)	5	25	20	⋯	40
Al	40 W (dc)	5	25	20	⋯	40
c-WO_3	35 W (dc)	15	375	35	4.5	160
a-WO_3	35 W (dc)	15	25	35	4.5	160
Ta_2O_5	100 W (rf)	13	375	20	7	350

culations were performed prior to device manufacturing as discussed in Refs. 2 and 16. The reflectance modulation was measured in the spectral region from 2 to 40 μm.

The spectrally dependent emittance modulation ΔE of the device was obtained from the experimentally measured reflectance modulation. The emittance of a nontransmitting device is defined $E = 1 - R$ (R = reflectance). The emissivity ϵ of the device in its different states (bleached, colored) relative to the blackbody spectra at $T = 300$ K is given by:

$$\epsilon = \frac{\int_{\lambda_1}^{\lambda_2}[1 - R(\lambda)]M_b(\lambda,T)d\lambda}{\int_{\lambda_1}^{\lambda_2}M_b(\lambda,T)d\lambda}, \tag{1}$$

where $R(\lambda)$ is the measured reflectance and $M_b(\lambda,T)$ is the blackbody spectral emittance. In this calculation the temperature was fixed at 300 K, and λ_1 and λ_2 were 2 and 40 μm, respectively. There are two important values characterizing the performance of an electrochromic device for thermal control. The device emissivity modulation $\epsilon_{modulation}$ and the ratio ϵ_{ratio} are given by the difference and the quotient of the emissivity in the devices high and low emittance state. For practical applications a low modulating device with a high ratio could be used as well as a high modulation device with a low ratio. Although for thermal emittance control a larger area of the object needs to be coated with an electrochromic active layer stack having a smaller modulation and a higher ratio than for a high modulation layer ensemble.

II. EXPERIMENT

The thin film all-solid state device constituent layers were deposited by dc or rf magnetron sputtering in a high-vacuum (HV) deposition chamber with a typical background pressure of 3×10^{-6} Torr. Glass slides were used as the substrate material. Table I gives deposition conditions of the various films used to manufacture the devices. *In situ* ellipsometry was used to monitor the layer growth, and to obtain growth rates. Polymer devices were manufactured by producing half-devices, which contained either the electrochromic, or the ion storage layer. The half devices were sandwiched together using the polymer layer.

Electrochemical Li^+ intercalation was performed in a 1.0 molar solution of $LiClO_4$ in propylene carbonate using a potentiostat. The electrochemical cell contained a platinum foil as a counter electrode and a saturated calomel reference electrode. The potentiostat controls the voltage at the working electrode (sample) by varying the counter electrode potential. The electrochemical Li^+ insertion for the all-solid-

state devices was introduced into the finished device structures through the top metal grid. In the polymer device both half devices were Li$^+$ intercalated before sticking them together.

The IR transmissive top and bottom electrode aluminum metal grids are made by photolithography. Two different sets of grid masks were used. The mask for grid 1 (fine grid) had a linewidth of 5 μm and a period of 100 μm, whereas the mask for grid 2 (coarse grid) was made for 10 μm linewidths and a 500 μm line period. The transmission was calculated to be 95% and 90% for grids 1 and 2, respectively.

Prior to assembling the devices, the constituent layers were deposited as single films onto [001] silicon substrates. Glancing-angle-of incidence x-ray diffractometry (XRD) was used to study the phase content and crystallinity of the thin films.[17,18]

The optical properties of all device constituents were investigated by spectroscopic ellipsometry in the spectral region from 0.03 to 8.5 eV (0.15–40 μm, vacuum ultraviolet to deep infrared).[17–19] In addition, the ellipsometry data were used to determine the spectrally dependent optical dielectric function as well as the thin-film microporosity. The optical response was also measured on ''half-devices,'' consisting of either substrate/electrode/electrochromic layer or substrate/electrode/ion storage layer.[14] With this assembly, we determined the change in the dielectric function of the electrochromic and ion storage layers after Li$^+$ insertion and extraction. The results from these optical investigations were used to build a virtual device structure, and the device emissivity modulation performance (emittance integrated over the blackbody spectrum) was simulated. In this way the device structure was optimized prior to experimental manufacture of the device.[16]

To study the reflectance modulation the finished real devices were electrically cycled between +2 V and −2 V. Reflectance spectra were measured in the spectral range from 2 to 40 μm using a Michelson FTIR spectrometer. Reflectance data were taken at an 11° angle of incidence.

III. MATERIALS

Polycrystalline WO$_3$ as-deposited films possess a monoclinic crystal structure (Fig. 1). An irreversible phase transformation occurred after Li$^+$ insertion, resulting in a cubic structure Li$_x$W$_{(1-x)}$O$_3$ (tungsten bronze) which changed to a tetragonal Li$_x$W$_{(1-x)}$O$_3$ modification after Li$^+$ extraction (Fig. 1). It has been shown elsewhere,[20] that the crystal structure of tungsten bronze is a function of Li concentration. According to the explanation given in Ref. 20 the irreversibility of the phase transformation is caused by a certain amount of Li$^+$, which remains in the WO$_3$ after ion extraction. The optical properties of bleached and colored polycrystalline tungsten oxide were analyzed using infrared ellipsometry. Single films of tungsten oxide were deposited onto [001] silicon wafers and measured after coloring and bleaching. The optical properties of colored and bleached polycrystalline tungsten oxide thin films are given in Fig. 2 in terms of the real (ϵ_1) and imaginary (ϵ_2) part of the dielectric function ϵ. In almost the entire spectral region ϵ_1 and ϵ_2 of
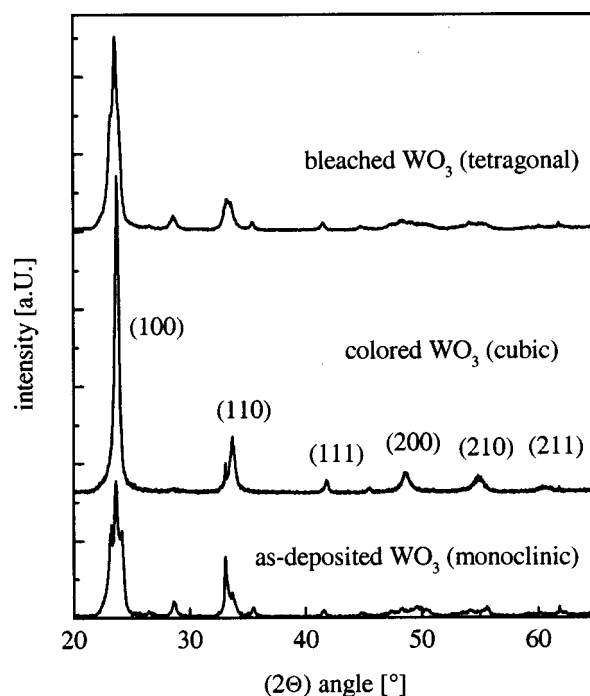

FIG. 1. Glancing-angle-of-incidence x-ray diffraction spectra taken from as-deposited, colored and bleached Li$_x$WO$_{3-x}$ single films on [001] Si.

the colored film is higher than that of the bleached film. There is a crossover in ϵ_2 near 25 μm. A phonon absorption was found in c-WO$_3$ near 14 μm. The amplitude for this absorption is much higher in the colored than in bleached c-WO$_3$.
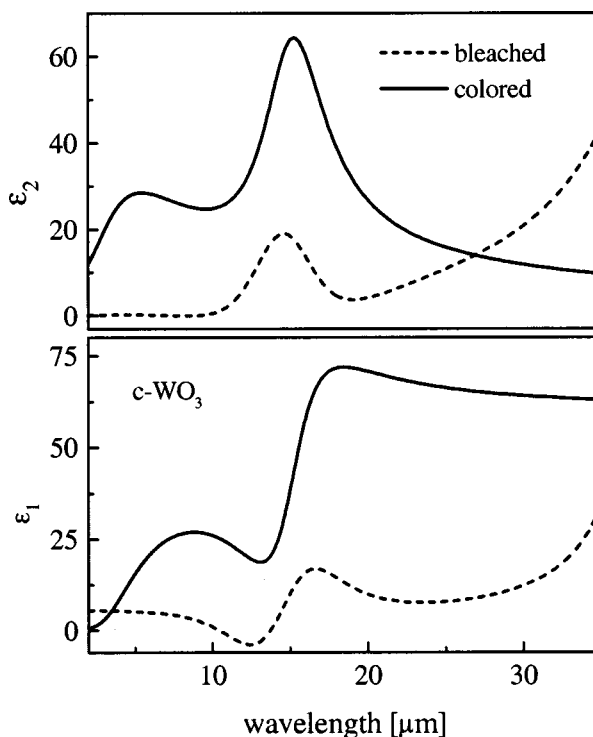

FIG. 2. IR dielectric function modulation of bleached/colored polycrystalline electrochromic Li$_x$WO$_{3-x}$ layer after ion extraction/insertion.
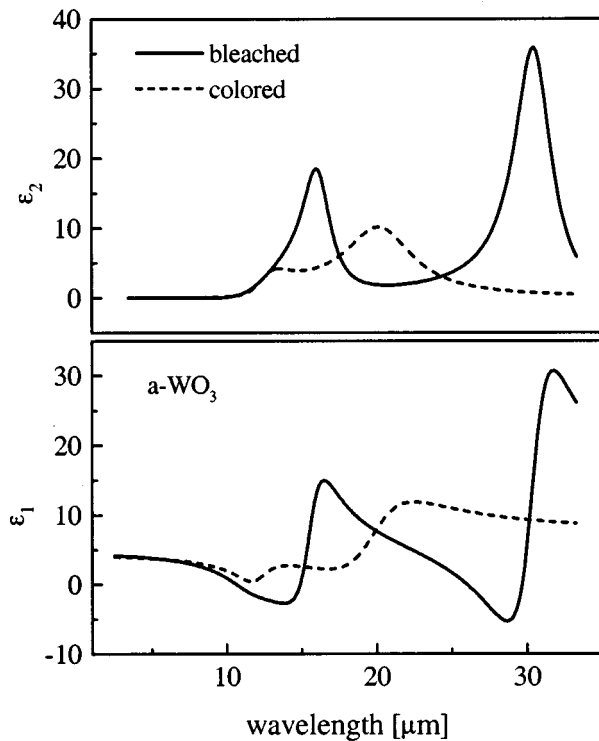
FIG. 3. IR dielectric function modulation of bleached/colored amorphous ion storage Li_xWO_{3-x} layer after ion extraction/insertion.

FIG. 4. IR dielectric function of the Ta_xO_y ion conductor.

Amorphous tungsten oxide (a-WO_3) thin films were deposited at room temperature, also on [001] silicon substrates. Their amorphous structure was verified by XRD measurements. Two phonon absorptions were found in the bleached a-WO_3 near 15 μm and near 30 μm (Fig. 3). The phonon absorptions became much weaker upon Li^+ intercalation and moved in spectral position to 13 and 20 μm, respectively. However even though there was a change in the optical properties of a-WO_3 upon Li^+ insertion and extraction, the ϵ_1 and ϵ_2 modulation is much weaker for a-WO_3 than for c-WO_3. The coloration effect after Li^+ insertion into a-WO_3 was also studied by Burdis *et al.*[21] using FTIR spectroscopy.

The tantalum oxide thin films were amorphous when deposited in our typical deposition regime. However the deposition process was optimized with respect to microporosity of the thin films. There are especially high quality requirements for the ion conductor layer material, because pinholes in this layer can cause unwanted electrical conductivity between the electrochromic and ion storage layers resulting in a failure in device operation. Tantalum oxide thin films deposited at temperatures higher than 200 °C and oxygen flux rates above 7 sccm showed a considerably smaller microporosity.[18] The optical properties of tantalum oxide thin films are given in Fig. 4.

ITO or aluminum (Al) was used as the electrode material. Electrically conducting materials have Drude-like optical behavior (free carrier effects) at long wavelengths. Thin film optical properties of ITO and Al were also determined by ellipsometry.
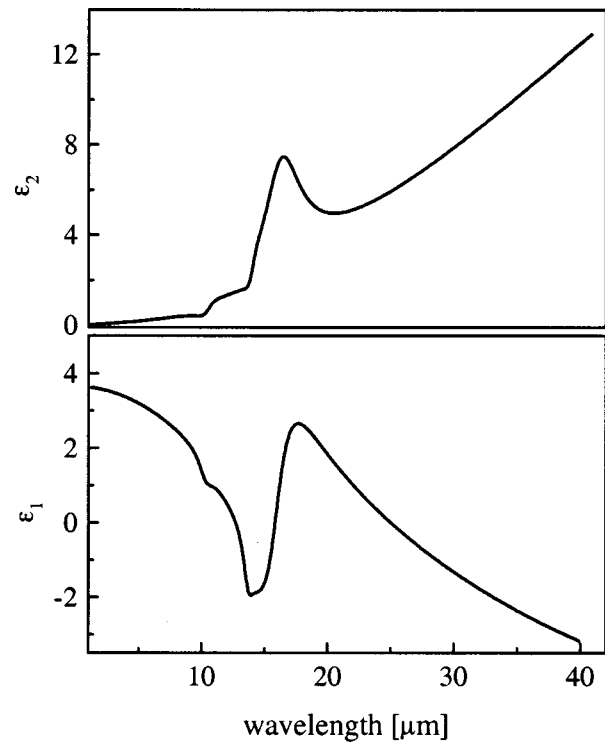
IV. RESULTS AND DISCUSSION

Prior to device manufacture we simulated the emittance modulation for devices with different layer structures. A possible structure for an all-solid state device is shown in Fig. 5. In this case the bottom electrode can be a coalescent aluminum metal layer (single-grid device) or an aluminum metal grid (double-grid device). The two device types function in different ways. Whereas the single-grid device operates on
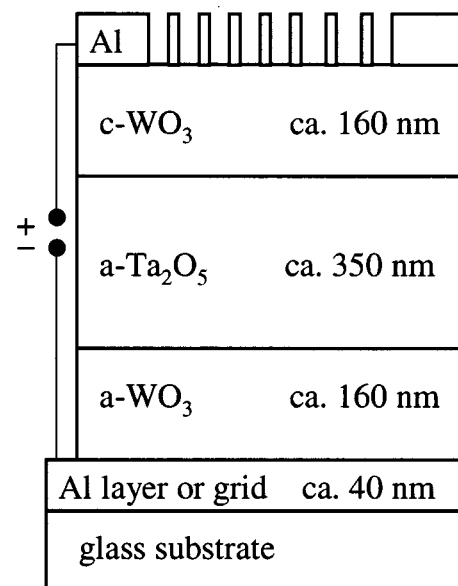

FIG. 5. Layer structure of the all-solid-state electrochromic devices for thermal emittance modulation in the spectral region from 2 to 35 μm. The bottom electrode consists of either a continuous Al metal layer or an Al metal grid.
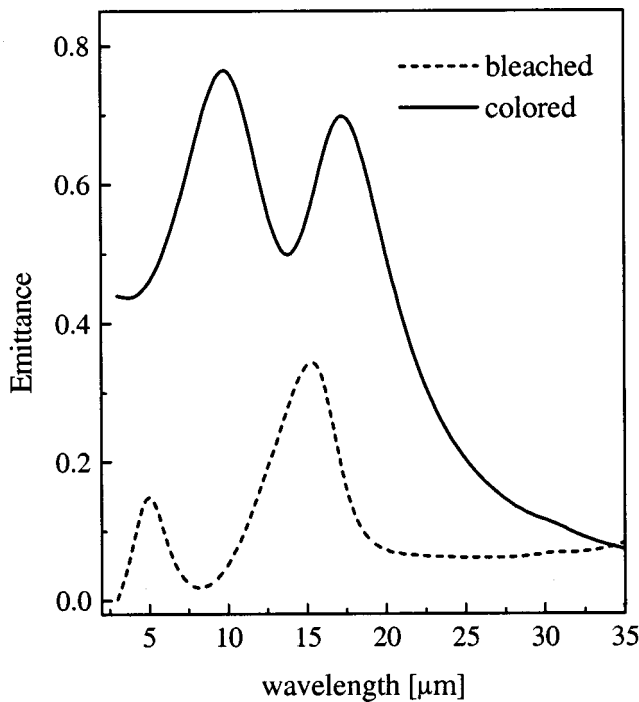
FIG. 6. Emittance modulation simulation in the spectral region from 2 to 35 μm for a single-grid electrochromic device with layer structure shown in Fig. 5.

FIG. 8. Emittance modulation of the single-grid electrochromic device for thermal emissivity modulation for wavelength from 2 to 40 μm.

the basis of reflectance modulation, the double-grid device works by modulation of the substrate emission. The results of the device performance simulations in terms of emittance modulation are given in Fig. 6 for the single-grid device, and in Fig. 7 for the double-grid all-solid state device. In the
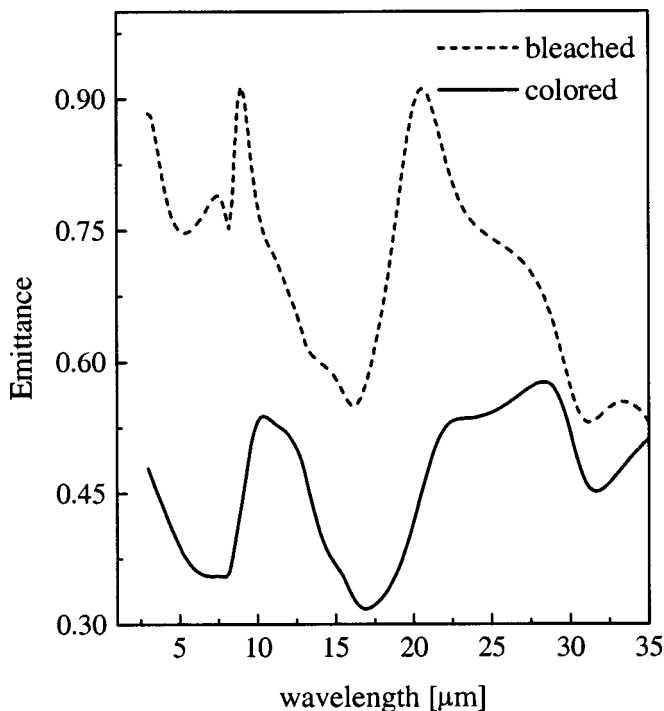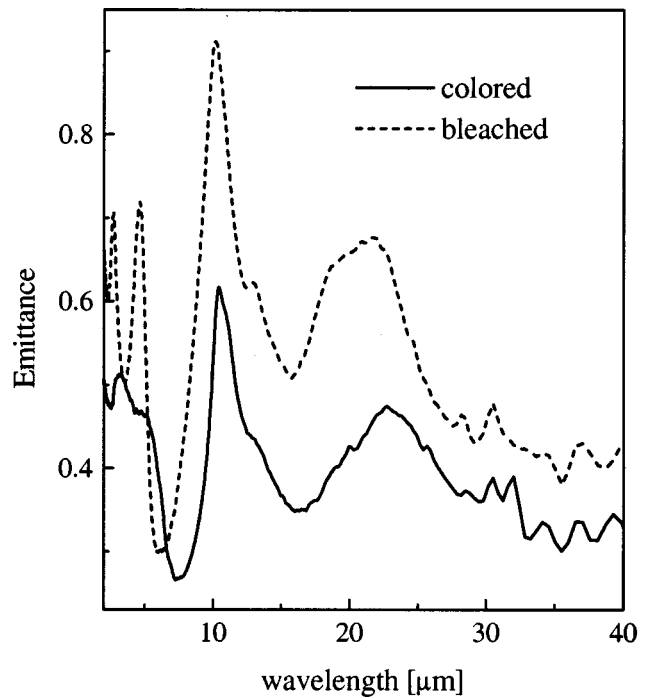
reflectance modulation based single-grid device the bleached state refers to the low emittance condition, and the colored state to the high emittance condition. The integrated emissivity ϵ [Eq. (1)] of the colored and bleached device states found from integration over the blackbody spectrum at 300 K are 0.45 and 0.88, respectively. This corresponds to a total emissivity modulation of 43% and an emissivity ratio of 1.94.

The double-grid device operates in the opposite way to the single-grid device. Here, the bleached state refers to the high emittance state, and the colored state represents the low emittance state. The integrated emissivity is calculated to be 0.28 and 0.56 for the colored and bleached state, respectively. The total emissivity modulation is 28% and therefore smaller than the emissivity modulation for the single-grid device. The emissivity ratio obtained was 1.98.

All-solid state electrochromic devices were manufactured according to the device structures proposed in the emittance modulation simulations. The emittance modulation of a single-grid device is given in Fig. 8. The devices were cycled between +2 V (bleached) and −2 V (colored) several times, reversibly reaching the low and high emissivity states. However devices exposed to atmosphere for more than two days lead to device failure. We assume that the Li^+ reacted with atmospheric nitrogen or oxygen and became immobile. There were strong lattice absorptions in the device response just above 10 μm. From IR optical data it is known that the characteristic lattice absorptions of the metal oxides (c-WO_3, a-WO_3, a-Ta_2O_5) are localized in this spectral region. These strong absorptions in the entire device are therefore due to a sum of lattice absorption contributions from each metal oxide layer. To improve device performance the absorption broadening can be reduced by using smaller layer

FIG. 7. Emittance modulation simulation in the spectral region from 2 to 35 μm for a double-grid electrochromic device with layer structure shown in Fig. 5.

thicknesses, or higher material perfection. There is additional reflectance modulation due to thickness interference effects in the spectral region from 15 to 40 μm, which are mainly caused by the a-Ta_2O_5 ion conductor layer. To remove these interference effects a thinner layer should be used. However, devices with thinner Ta_2O_5 layer thickness usually failed because of electrical shorts between ion storage and electrochromic layers. Further attempts to improve the ion conductor structural properties should help solve this problem and allow optimizing the Ta_2O_5 layer thickness to limit interference effects.

The emissivity in the low- and the high-emittance state integrated over the 300 K blackbody spectra was calculated from the reflectance spectra measured in the devices bleached and colored states, and found to be 0.4 and 0.58, respectively. This results in emissivity modulation of 18% and an emissivity ratio of 1.45. This is a much lower emissivity modulation than expected from our simulations. One reason might be a nonuniform Li^+ depth distribution. Thus a Li^+ depth profile was measured by secondary neutral mass spectroscopy (SNMS). The SNMS profile showed a high concentration of Li^+ captured at each interface between adjacent layers. It also showed a nonuniformity in the Li distribution which had a concentration maxima at the interfaces and minima in the middle of the layer. After device switching a certain amount of Li^+ always remained in the layer (electrochromic or ion storage) which was supposed to be Li free, or it was stacked in the tantalum oxide ion conductor layer. The nonideal Li distribution is likely the major difference between the idealized simulated device performance and the real experiments.

The modulation performance of the single-grid device also did not follow predictions from simulations. In the simulation it was shown that the device bleached and colored states refer to the low and high emissive conditions, respectively. However, the single-grid device performance experimentally shows the opposite behavior. An explanation could be that a certain amount of Li^+ ions remain in the electrochromic layer after ion extraction and the device switches only between a higher and a lower reflecting electrochromic top c-WO_3 layer. If this is the case incident light may not reach the bottom electrode where it should be reflected in the devices bleached state according to our simulations.

The performance of a double-grid electrochromic device is given in Fig. 9. Again there was a strong absorption due to phonon vibrations centered just above 10 μm, and absorptions due to thickness interference effects. The integrated emissivity of the device in its bleached and colored states was calculated to be 0.8 and 0.64. This resulted in an emissivity modulation of 16% and an emissivity ratio of 1.26. The double-grid device had a somewhat smaller performance range than the single-grid device predicted by simulations. However, in the case of the double-grid device the modulation followed the same switching behavior as shown in the simulations, having the bleached and the colored states as the high and low emissive conditions, respectively. The difference in the dynamic modulation range between simulation and experiment can be explained in the same way as for the
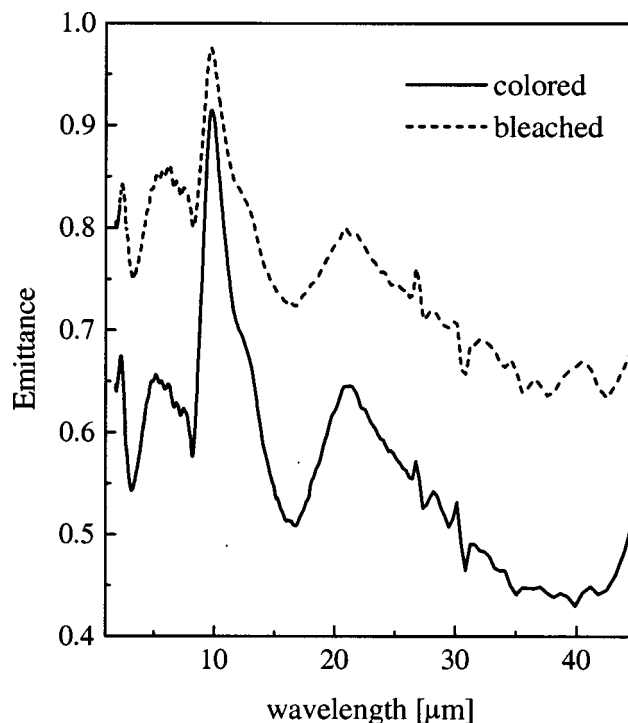

FIG. 9. Emittance modulation of the double-grid electrochromic device for thermal emissivity modulation for wavelength from 2 to 45 μm.

single-grid device, namely that ions possibly do not move uniformly between layers.

c-WO_3 has been exposed to atomic oxygen under UV radiation in order to test the materials reliability in space environment. Investigations showed a degradation and a blue coloring of c-WO_3. For that reason a simulation was made to test the electrochromic device performance with a protection layer on top of the top electrode metal grid. The same device structure was used as for the single-grid device modulation simulations. Several materials have been tested in the simulation, whereas a 600 nm ZnS coating showed the most promising optical switching results (Fig. 10). According to the simulation the overcoat layer fulfills a twofold purpose; first it serves as a protection layer for the highly reactive Li^+ and c-WO_3, and second it improves the device performance in the spectral region of interest. For a ZnS overcoat the emissivity integrated over the 300 K blackbody was calculated to be 0.61 and 0.13 in the devices colored and bleached states, which results in an emissivity modulation of 48% and an emissivity ratio of 4.56. Similar simulations have been performed using 900 nm thick MgF_2 as a device cap layer, since there are some doubts about the stability of ZnS in space. MgF_2 is a material often used for optical coatings and easy to deposit. Simulated performance of a device with a MgF_2 overcoat is shown in Fig. 11. MgF_2 is uniaxial, and both ordinary and extraordinary optical constant spectra were isotropic averaged to simulate the optical response of a polycrystalline layer with randomly oriented grains. The emissivity modulation again integrated over the 300 K blackbody was obtained to be 29% and the emissivity ratio was 2.82. As can be seen in Fig. 11 the modulation maximum for a MgF_2 covered device is near 6 μm therefore this kind of device is
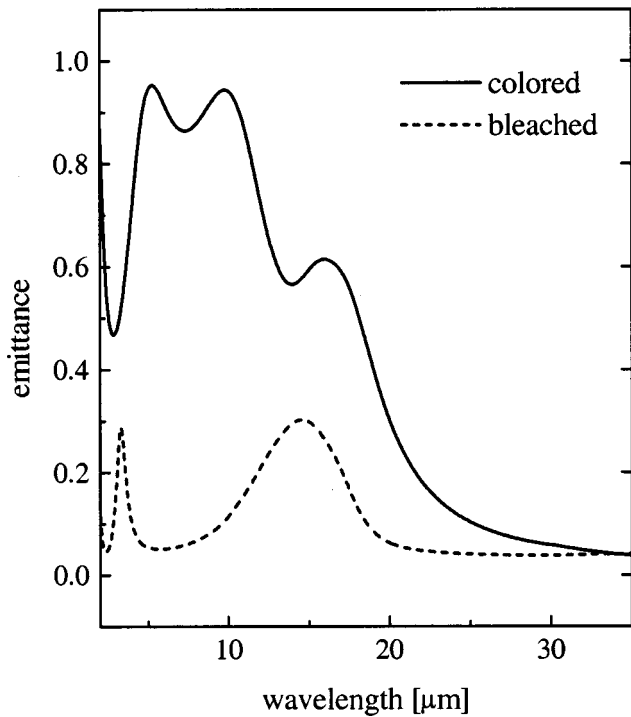
FIG. 10. Simulated device performance for a single-grid electrochromic device with a ZnS protection coating on top of the Al metal grid.

FIG. 12. Layer structure of the polymer electrochromic device for thermal emittance modulation in the spectral region from 2 to 35 μm. A DLC anti-reflecting coating is deposited on top of the slightly doped silicon substrate to improve the emissivity modulation.

just right for high temperature applications. Emissivity modulation and ratio calculated by integration over the 600 and 900 K blackbody spectra were obtained to be 52% and 4.88, and 50% and 5.2. Space stability of MgF_2 will be investigated in the future by sample exposure to atomic oxygen and UV radiation in a special plasma chamber.
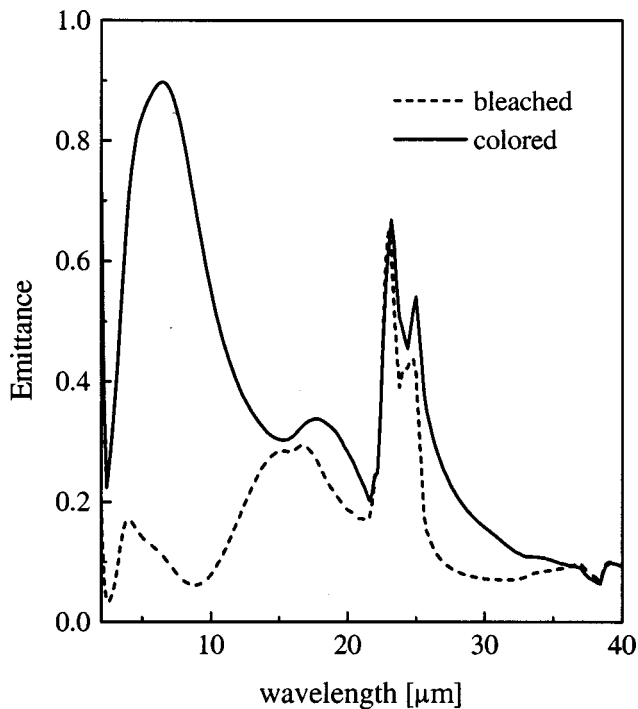
A third structure for an emissivity modulating electrochromic device is shown in Fig. 12. Here a highly absorbing/emissive AMPS/DMA polymer ion conductor was used. A DLC coating was deposited on top of the low-doped silicon substrate to improve device performance. For this device type the emissivity modulation was caused only by the change in optical properties of the c-WO$_3$-top layer, since

FIG. 11. Simulated device performance for a single-grid electrochromic device with a MgF$_2$ protection coating on top of the Al metal grid.
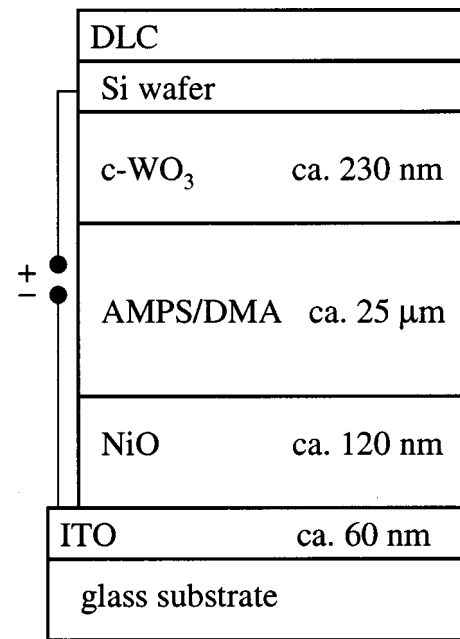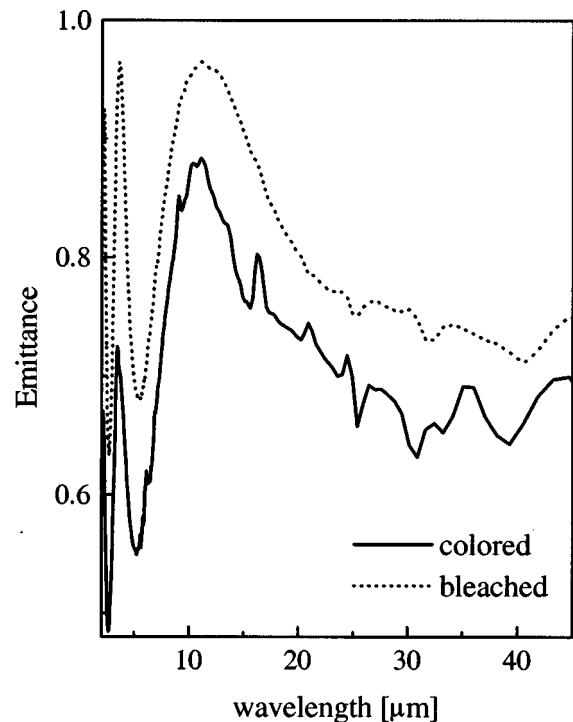
FIG. 13. Emittance modulation of the polymer electrochromic device for thermal emissivity modulation for wavelength from 2 to 45 μm.

TABLE II. Calculated and experimentally measured device performance for the single and double-grid all-solid state devices and the polymer device; $\epsilon_{bleached}$ and $\epsilon_{colored}$ are the calculated emissivity values of the device in its bleached and colored states integrated over the 300 K blackbody spectra, ϵ_{ratio} and $\epsilon_{modulation}$ give the ratio and the difference between the high and the low emissivity states of the device.

Device type	$\epsilon_{bleached}$	$\epsilon_{colored}$	$\epsilon_{modulation}$ (%)	ϵ_{ratio}
Single-grid simulation device	0.45	0.88	43	1.94
Double-grid simulation device	0.56	0.28	28	1.98
Single-grid experimental device	0.58	0.4	18	1.45
Double-grid experimental device	0.8	0.64	16	1.26
Single-grid simulation device with ZnS coating	0.13	0.61	48	4.56
Single-grid simulation device with MgF$_2$ coating (300 K blackbody)	0.17	0.46	29	2.66
Single-grid simulation device with MgF$_2$ coating (600 K blackbody)	0.13	0.65	52	4.88
Single-grid simulation device with MgF$_2$ coating (900 K blackbody)	0.12	0.62	50	5.2
Polymer experimental device	0.86	0.76	10	1.1

the layers underneath the absorbing ion conductor could not contribute to the reflectance spectra of the device. The experimental effort needed to manufacture this device type is higher than for the all-vacuum-solid state devices. The emittance modulation for the polymer device is given in Fig. 13. The emissivity for the bleached and colored states integrated over the 300 K blackbody is 0.86 and 0.76, respectively, corresponding to an emissivity modulation of 10% and an emissivity ratio of 1.1. The calculated values for simulated and experimentally measured device performances for all three device types are summarized in Table II.

V. CONCLUSIONS

The design and performance of three different types of EMDs, two all-solid state devices (single- and double-grid device) and a polymer-based device have been discussed. Polycrystalline c-Li$_x$W$_{1-x}$O$_3$ and amorphous a-Li$_x$W$_{1-x}$O$_3$ (or NiO for the polymer device) have been used as electrochromic and ion storage layers, respectively. Tantalum oxide was used as an ion conductor in the all-solid state devices. The infrared optical constants for all device constituents have been obtained by spectroscopic ellipsometry. The results have been used to model virtual devices, thus allowing simulation of the reflectance modulation between the colored and bleached states of the device and thereby predicting the device performance. These devices were experimentally manufactured and had the same structure as used for the simulations. The range of device operation was investigated

for the spectral region from 2 to 40 μm. The simulated and experimentally measured reflectance spectra in the spectral region from 2 to 40 μm were used to calculate the emissivity modulation of the device integrated over the 300 K blackbody emissivity spectra. Simulations and experiment showed the best device performance for the single-grid device, although simulations predict an opposite switching behavior than found experimentally. The double-grid device emissivity modulation was mostly limited by the strong phonon absorption near 10 μm, which is unfortunately just above the peak maximum of the 300 K blackbody spectra. All devices introduced in this work were switched for several cycles, reaching the low and high emissive state reversibly.

[1] C. G. Granqvist, *Handbook of Inorganic Electrochromic Materials* (Elsevier, Amsterdam, 1995).
[2] C. L. Trimble, E. Franke, J. S. Hale, and J. A. Woollam, *Proceedings of Space Technology and Applications International Forum*, edited by M. S. El-Genk (2000), p. 797.
[3] A. G. Darrin, R. Osiander, J. Champion, T. Swanson, and D. Douglas, *Proceedings of Space Technology and Applications International Forum*, edited by M. S. El-Genk (2000), p. 803.
[4] L. M. Grob and T. D. Swanson, *Proceedings of Space Technology and Applications International Forum*, edited by M. S. El-Genk (2000), p. 809.
[5] D. G. Gilmore, *Satellite Thermal Control Handbook* (The Aerospace Corporation, El Segundo, CA, 1994), p. 4.
[6] R. B. Goldner and R. D. Rauh, Proc. SPIE **428**, 38 (1983).
[7] R. B. Goldner, F. Arntz, G. Berera, T. E. Haas, G. Wei, K. K. Wong, and P. Yu, Proc. SPIE **1536**, 34 (1991).
[8] S. F. Cogan, T. D. Plante, M. A. Parker, and R. D. Rauh, J. Appl. Phys. **60**, 2735 (1986).
[9] S. F. Cogan, R. D. Rauh, J. D. Klein, and T. D. Plante, Proc. SPIE **1149**, 2 (1989).
[10] C. G. Granqvist, Sol. Energy Mater. Sol. Cells **60**, 201 (2000).
[11] C. G. Granqvist, Appl. Phys. A: Solids Surf. **52**, 83 (1991).
[12] K. Baucke, Sol. Energy Mater. **16**, 67 (1987).
[13] P. Topart and P. Hourquebie, Thin Solid Films **352**, 243 (1999).
[14] C. L. Trimble, M. J. DeVries, J. S. Hale, D. W. Thompson, T. E. Tiwald, and J. A. Woollam, Thin Solid Films **347**, 1 (1999).
[15] S. F. Cogan, R. D. Rauh, J. D. Klein, and T. D. Plante, *Electrochemical Society Proceedings* (Electrochemical Society, Pennington, NJ, 1995), Vol. 94-2, p. 269.
[16] J. S. Hale and J. A. Woollam, Thin Solid Films **339**, 174 (1999).
[17] M. J. DeVries, C. L. Trimble, T. E. Tiwald, D. W. Thompson, J. A. Woollam, and J. S. Hale, J. Vac. Sci. Technol. A **17**, 2906 (1999).
[18] E. Franke, M. Schubert, C. L. Trimble, M. J. DeVries, J. S. Hale, J. A. Woollam, and F. Frost, J. Appl. Phys. (submitted).
[19] J. S. Hale, M. J. DeVries, B. Dworak, and J. A. Woollam, Thin Solid Films **313–314**, 205 (1998).
[20] Q. Zhong, J. R. Dahn, and K. Colbow, Phys. Rev. B **46**, 2554 (1992).
[21] M. S. Burdis, J. R. Siddle, and S. Taylor, Proc. SPIE **2255**, 371 (1994).